Long-lived Triplet Excited State in a Heterogeneous Modified Carbon Nitride Photocatalyst

Adam J. Rieth, Yangzhong Qin, Benjamin C. M. Martindale, and Daniel G. Nocera*

Department of Chemistry and Chemical Biology, Harvard University, 12 Oxford St. Cambridge, MA 02138

ABSTRACT: Heterogeneous carbon nitrides have numerous advantages as photocatalysts, including strong light absorption, tunable band edges, and scalability, but their performance and continued development are limited by fast charge recombination and an under-developed mechanistic understanding of photodriven interfacial electron transfer. These shortcomings are a result of complex photophysics leading to rate asynchrony between oxidation and reduction, as well as redox processes driven out of electronic trap states rather than excited states. We show that a well-defined triplet excited state in cyanamide-modified carbon nitride is realized with appropriately sized particles. The utility of this long-lived excited state is demonstrated by its ability to drive a hydroamidation photoredox cycle. By tuning the particle size of CN_x, the oxidation-reduction photochemistry of carbon nitride may be balanced to achieve a redox-neutral closed photocatalytic cycle. These results uncover a triplet excited state chemistry for appropriately sized CN_x particles that preludes a rich energy and electron transfer photochemistry for these materials.

INTRODUCTION

Long-lived triplet states enable a rich photochemistry by affording a well-defined excited state energy and a long enough lifetime to enable reactivity on the timescale of diffusion. Whereas triplet excited states are customary for molecular species, such excited states for heterogeneous photoreagents are less common, especially for semiconductors where the excited state dynamics may be dominated by trap states. Such is the case for carbon nitride (CN_x),[1] which is capable of promoting a variety of light-driven redox processes such as hydrogen evolution,[2,3] alcohol oxidation,[4,5] as well as many organic transformations.[6−9] CN_x photoreagents have numerous advantages, including ease of product separation, scalability,[10] and the ability to tune band gap energies.[11] However, the efficiency of CN_x photoprocesses, and especially those that are redox-based, is widely acknowledged to be very low,[3,12] limited by charge recombination via nonradiative pathways as well as prompt fluorescence on a ~10 ns timescale[13,14] and redox processes driven out of electronic trap states[15−18] rather than from the conduction band. These two limitations have largely prohibited the use of CN_x in photocatalytic cycles requiring diffusive exciton quenching, as well as prevented a well-defined mechanistic analysis of photoredox cycles.

Efforts to circumvent the inefficiency arising from trap states in heterogeneous CN_x materials include methods to incorporate double-bonded heteroatoms as terminating groups. Heteroatom incorporation can remove trap states on the surface as well as result in longer-lived triplet excitons in melon ($^{NH_2}CN_x$, Figure 1, top) by accelerating intersystem crossing (ISC).[19−21] However, the population of the excited state triplet remains restricted by the slow rate of ISC relative to fluorescence relaxation, and, quizzically, direct quenching of a triplet excited state in CN_x has not been observed. In the absence of emissive quenching, together with the insensitivity of CN_x singlet fluorescence to charge transfer processes,[13,14] CN_x photoreactivity has largely been ascribed to lower-energy trap-states.[15] Redox processes driven out of trap states make CN_x materials competent photocatalysts for reactions that can tolerate disparate initial rates of oxidation versus reduction. This rate asynchrony as well as the fast charge recombination results in a frequent requirement for a sacrificial reagent to trap either the hole or electron equivalent, depending on the nature of the desired substrate conversion, to drive turnover within the photocycle. Excess trapped electrons resulting from faster initial hole quenching are reflected by a blue hue of cyanamide-modified $^{NCN}CN_x$ under irradiation in the presence of sacrificial reductants. This buildup of trapped electrons has been shown to accelerate charge recombination to ~10 ps,[15] which further decreases the efficiency of photocatalytic processes such as hydrogen evolution, as well as precludes any possibility of diffusive excited state quenching. To overcome these inefficiencies of fast fluorescence charge recombination and redox processes driven out of trap states, the tuning of CN_x to achieve more efficient triplet formation will increase the scope and applicability of CN_x as a photoreagent.

A well-defined photochemistry arising from a long-lived triplet state in a heterogeneous photocatalyst is exceptionally useful for organic photoredox. Photoredox methods comprise a powerful strategy to access unique reactive intermediates,[22−25] enabling novel cross couplings,[26−28] as well as asymmetric[29−32] and C–H activation transformations.[33−37] Organic photoredox cycles have largely relied on homogeneous Ru(II) or Ir(III) photocatalysts that are ideally suited for supporting radical-initiated pathways derived from one-electron quenching of long-lived triplet excited states.[38,39] More recently, heterogeneous photocatalysts such as CN_x have been explored as attractive replacements for molecular photocatalysts[6,7,11]

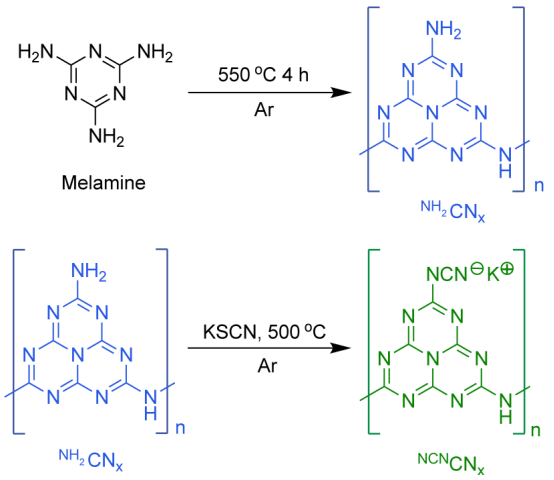

Figure 1. Cyanamide-modified $^{NCN}CN_x$ is synthesized via thermal KSCN treatment of $^{NH_2}CN_x$, which is accessible from the thermal decomposition of melamine.

because the materials can be separated and recycled, thereby avoiding contamination of products with heavy metals. Further, light absorption and redox properties may be easily tuned by choosing a semiconductor photocatalyst with a desired band gap.[40–46] However, for numerous closed, net redox-neutral photocycles, a long-lived triplet excited state is optimal to allow for diffusive excited-state quenching and avoid rate asynchrony between redox processes.

Here we report a long-lived triplet CN_x excited state accessed with size-controlled and surface-modified materials. Stable suspensions of these CN_x systems exhibit a rapidly decaying singlet excited state (τ_{fluor} ~ 9 ns) that is accompanied by a long-lived triplet emissive state (τ_{phos} ~ 1.77 μs), and accordingly is efficiently quenched by oxygen. We demonstrate the direct utility of this triplet excited state in CN_x to drive photoredox chemistry, exemplified here by a closed, redox-neutral hydroamidation photocycle.

RESULTS

CN_x Variants. Melon ($^{NH_2}CN_x$) was the synthon for CN_x variants and prepared according to Figure 1 (top). $^{NH_2}CN_x$ was modified by annealing in the presence of KSCN,[3] to form $^{NCN}CN_x$ (Figure 1, bottom) with an observable cyanamide stretch by infrared absorption spectroscopy (IR) at ~2200 cm^{-1} (Figure S1). $^{urea}CN_x$ was synthesized by acid-treatment of $^{NCN}CN_x$,[13] resulting in changes to the N–H stretching region in IR spectroscopy, as well as a blue-shifted band edge in diffuse reflectance UV-visible (DRUV-vis) spectroscopy, indicating an increased band gap energy of approximately 0.2 eV (Figures S1, S2, and S3B). Thermal treatment of $^{NH_2}CN_x$ in a KCl/LiCl eutectic[47] formed $^{KCl}CN_x$, which, by IR and X-ray photoelectron spectroscopy (XPS) was similar to $^{NCN}CN_x$, exhibiting an identical cyanamide IR stretch at ~2200 cm^{-1} as well as a potassium signal in XPS (Figures S1 and S5), but exhibited a red-shifted DRUV-vis band edge (Figure S3B). Mesoporous carbon nitride $^{mpg}CN_x$ was synthesized using a hard silica template by thermal treatment of melamine, followed by NH_4F etching, as previously reported.[44]

Photophysics. Time-resolved emission quenching and lifetime decay kinetics provide valuable handles for probing CN_x photocatalysis. For these measurements, suspending CN_x derivatives in organic solvents proved challenging. We therefore explored methods to reduce the CN_x particle size to achieve more stable suspensions. Previous attempts to gain bottom-up control of the degree of CN_x polymerization[48] resulted in materials that exclusively absorb UV light, thus limiting the utility of this method for photoredox applications. By contrast, top-down ball-milling of melon ($^{NH_2}CN_x$) resulted in much smaller (~20 nm) absorption blue-shifts as CN_x particle size is reduced,[49] with the band edge remaining in the visible region. Cyanamide modification of $^{NH_2}CN_x$ via thermal KSCN treatment was previously shown to increase the efficiency of photocatalytic processes as well as slightly red-shift light absorption.[3] We therefore examined the effects of particle size on cyanamide-modified carbon nitride ($^{NCN}CN_x$). The particle size of as-synthesized CN_x material was reduced via liquid-assisted grinding in a planetary ball-mill. After fractional size separation by centrifugation, CN_x materials with *Z*-average particle sizes, as measured by dynamic light scattering (DLS), of 304 nm ($^{NCN}CN_x^{304}$) and 148 nm ($^{NCN}CN_x^{148}$) were obtained, as compared to the 607 nm as-synthesized, parent material ($^{NCN}CN_x^{607}$) (Figure 2A). As previously observed for $^{NH_2}CN_x$, decreasing the particle size of $^{NCN}CN_x^{607}$ by ball-milling marginally affected the position of the band edge, resulting in a blue shift in the DRUV-vis of approximately 10 nm for both 304 nm and 148 nm fractions. Based on this change in absorption, the direct optical band gap shifts by only 0.06 eV, as determined from a Tauc plot[50] (Figure S3A). Notably, the absorption shoulder near 550 nm in $^{NCN}CN_x^{607}$ is absent after ball-milling (Figure 2B). This shoulder was previously attributed to

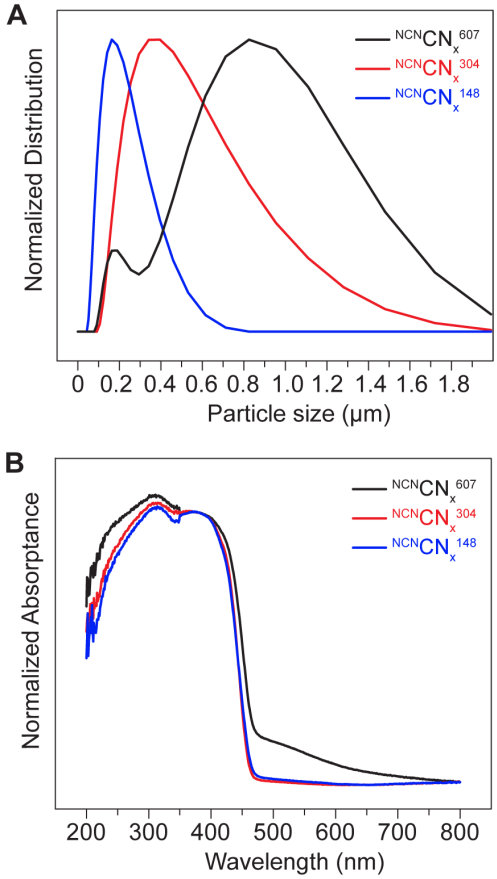

Figure 2. (**A**) Particle size distributions, as measured by DLS, for as-synthesized $^{NCN}CN_x^{607}$ (black) and two fractions after ball-milling (red and blue) with their corresponding *Z*-average diameters. (**B**) Normalized DRUV-vis absorptance (1 – reflectance) for $^{NCN}CN_x^{607}$ (black), $^{NCN}CN_x^{304}$ (red) and $^{NCN}CN_x^{148}$ (blue) ball-milled fractions.

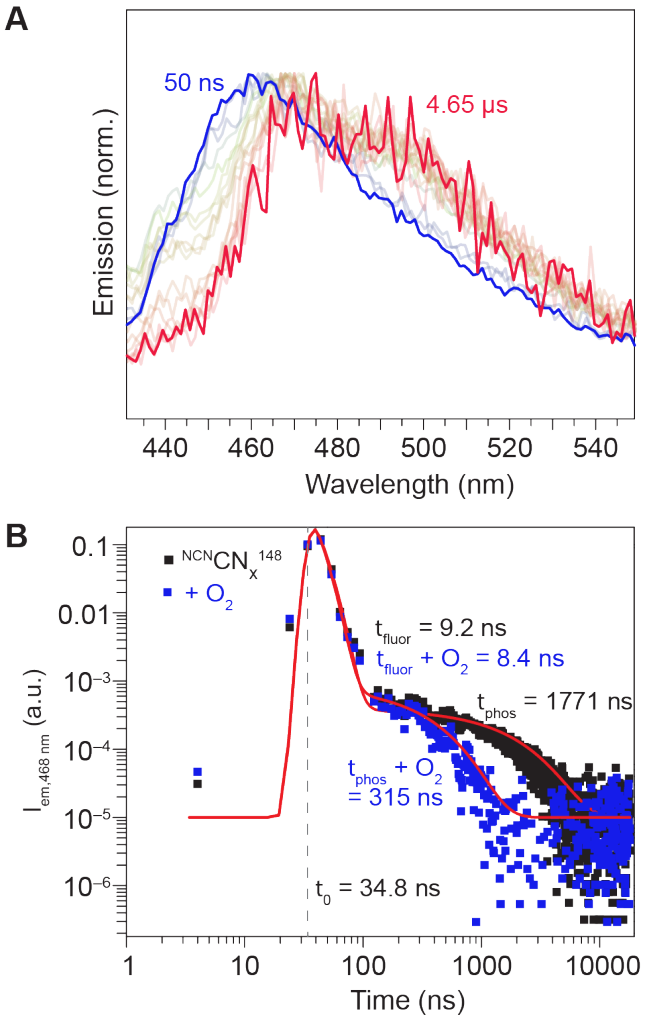

Figure 3. (**A**) Normalized emission spectral evolution from 50 ns to 4.65 µs for $^{NCN}CN_x^{148}$ excited at 355 nm. (**B**) Emission decay at 468 nm while exciting at 355 nm; red line shows the biexponential fit with corresponding lifetimes.

charge transfer excitation from heptazine to terminal cyanamide groups.[2] Although the shoulder disappears, the NCN modification is preserved as indicated by the similarity of the IR (the cyanamide stretch at 2200 cm^{-1} is retained) (Figure S1). Additionally, no significant changes are apparent by powder X-ray diffraction (PXRD) (Figure S7), nor in steady-state emission measurements (Figure S8), though a slight increase in the O1s signal is observed by XPS (Figure S4).

Reducing the particle size of $^{NCN}CN_x$ allowed for the formation of stable suspensions in organic solvent, enabling investigation of the photophysics via time-resolved emission spectroscopy. A long-lived emissive state was substantially more prominent for $^{NCN}CN_x^{148}$ than for $^{NCN}CN_x^{607}$ (Figure S9). Because $^{NCN}CN_x^{607}$ particles settle resulting in a greater inhomogeneity of the suspension, the data quality is not sufficient to achieve a high-quality fit for the long-lived emissive state. Interrogating the ns-resolved emission of $^{NCN}CN_x^{148}$ in suspension under a nitrogen atmosphere revealed a biphasic decay on distinct timescales. A fast process with a lifetime of τ_{fluor} = 9 ns was responsible for the majority of the emission intensity, consistent with previous lifetime measurements of CN_x in aqueous solution or in the solid state.[14,20,21] However, a slightly red-shifted (Figure 3A) long-lived emissive state with τ_{phos} =1.77 µs was also

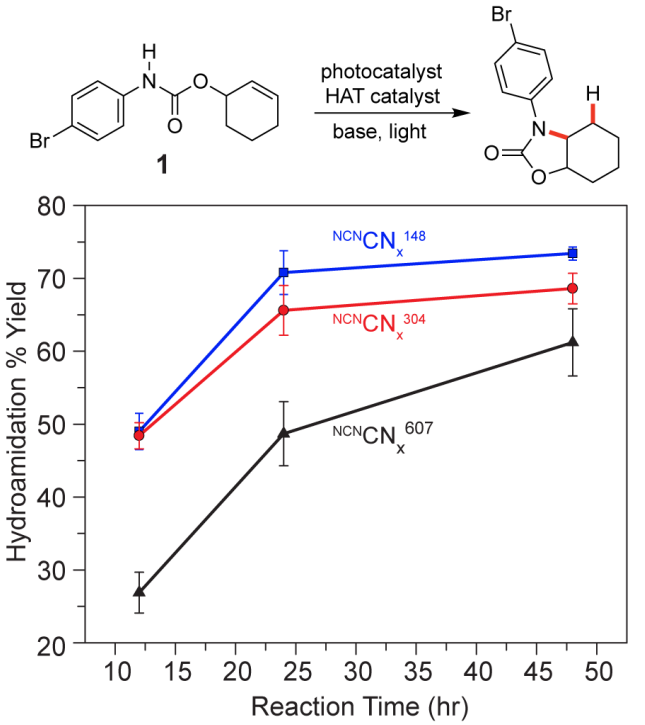

Figure 4. (top) Intramolecular hydroamidation reaction scheme for **1**, studied herein using carbon nitride (CN_x) photocatalysts. (bottom) Hydroamidation percent yield to product for **1** as a function of reaction time and particle size. Error bars represent standard error over 3 separate reactions.

observed (Figure 3B). Exposing the solution to air resulted in quenching of this long-lived emission, consistent with a phosphorescent triplet state; as expected, the prompt fluorescence was largely unperturbed in air (Figure 3B, blue). Additionally, cooling the suspension of $^{NCN}CN_x^{148}$ resulted in increased emission intensity on a long timescale of 4.8 µs (Figure S10), data which is inconsistent with a thermally activated emissive process, but expected for a phosphorescent triplet state.

Hydroamidation Reactivity. The observation of a long-lived luminescence that is quenched by O_2 is indicative of a triplet excited state, which we posited could be utilized to drive redox-neutral photocatalytic processes. To assess this contention, we examined a variety of CN_x variants as photocatalysts for the hydroamidation of olefins.

As-synthesized modified carbon nitride materials $^{NCN}CN_x$, $^{KCl}CN_x$, and $^{mpg}CN_x$ were marginally effective as photocatalysts for the intramolecular hydroamidation of 2-cyclo-hexen-1-yl(4-bromophenyl)carbamate (**1**) in the presence of 1 equiv phenyl disulfide (PhSSPh) and 0.2 equiv tributylmethylammonium dibutylphosphate (P_i^{Bu2}), and illuminated by a single blue LED light (Figure 4, top). $^{NCN}CN_x$, $^{KCl}CN_x$, and $^{mpg}CN_x$ each gave improved yields when compared to acid-treated $^{urea}CN_x$, and substantially improved over unmodified $^{NH_2}CN_x$ (Figure S6A). A blue coloration was observed during the reaction when using $^{NCN}CN_x$ and $^{KCl}CN_x$, consistent with previous reports of trapped, long-lived mid-gap electrons during the reaction.[15,16]

Ball-milling treatment and reduction of the particle size of $^{NCN}CN_x$ substantially accelerated the reaction rate for hydroamidation. After 24 h, intramolecular hydroamidation of **1** proceeded in 70.8% product yield, or 80.5% yield based on recovered starting material (BRSM), for $^{NCN}CN_x^{148}$ in the presence of 1 equiv bis(2,4,6-

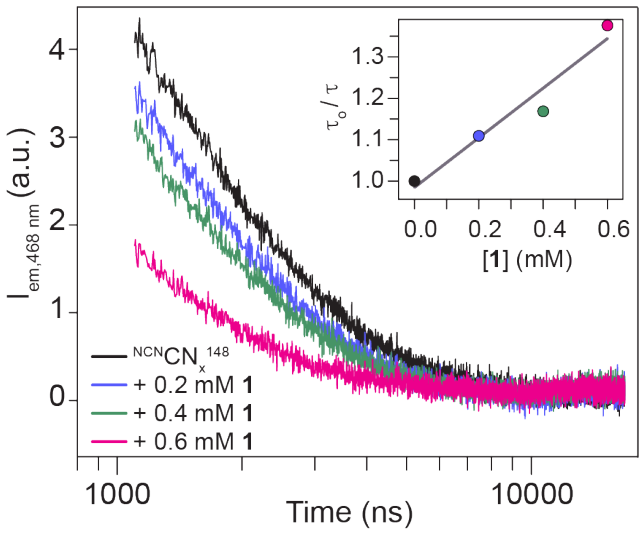

Figure 5. Emission decay of $^{NCN}CN_x^{148}$, measured at 468 nm with 0, 0.2, 0.4, and 0.6 mM of **1** and 1 mM P_i^{Bu2}. The data were truncated before 1000 ns to focus on the long-lived emission. Fits to the data are presented in the Supporting Information. (Inset) Stern-Volmer analysis of lifetime decays (τ_o = 1.55 μs) yields K_{sv} = 599 M^{-1} and k_q = 3.87 × 10^8 M^{-1} s^{-1}.

trimethylphenyl) disulfide (MesSSMes), 0.2 equiv P_i^{Bu2}, and illuminated by two blue LED lights. In the absence of base, using $^{NCN}CN_x^{148}$ over 24 hours resulted in 31% yield (BRSM), and in the absence of light, 0% yield. The hydroamidation conversion yield obtained from $^{NCN}CN_x^{148}$ and $^{NCN}CN_x^{304}$ are significantly improved compared with as-synthesized $^{NCN}CN_x^{607}$ (Figures 4 and S6B). We note the yields based on recovered starting material (BRSM, Figure S6B) are slightly higher (~5–10% for $^{NCN}CN_x^{148}$ and $^{NCN}CN_x^{304}$ and ~2% for $^{NCN}CN_x^{607}$) than those determined with an internal standard (Figure 4). This discrepancy in remaining starting material between the smaller particle sized $^{NCN}CN_x$ (i.e., higher surface area) suggests that a minor component of starting material is lost either by adsorption to the surface or by intermediate radicals in the photocycle of Figure 6 reacting with the surface of $^{NCN}CN_x$.

We note that excitation of a dichloromethane solution of MesSSMes, in the absence of any photocatalyst, at 430 nm using a ns-resolved transient absorption laser spectroscopy setup revealed the formation of MesS•, as evidenced by a long-lived absorbance at 490 nm (Figure S15). Examination of the UV-vis spectrum of MesSSMes reveals an absorbance in the UV, with a tail extending to approximately 440 nm (Figure S15, inset). Based on these results, it is likely that under reaction conditions of blue LED light, MesS• can be formed from direct photocleavage of MesSSMes.

Hydroamidation Kinetics We initially examined the emission quenching of $^{NCN}CN_x$ by hydroamidation reaction components using a fluorometer, which measures the steady-state emission intensity without time resolution. We observed no quenching of the $^{NCN}CN_x$ emission intensity when substrate **1** was added in combination with phosphate base (Figure S11).

To delve deeper into the mechanism of hydroamidation in the absence of steady-state emissive quenching, we examined the emission using ns-resolved laser spectroscopy. Titration of a $^{NCN}CN_x^{148}$ suspension with carbamate substrate **1** in the absence of base resulted in no change to the emission lifetime (Figure S12). However, in the presence of 1 mM P_i^{Bu2}, the emission lifetime of the long-lived state decayed upon addition of carbamate substrate with an apparent K_{sv} = 599 M^{-1}. In combination with the 1.55 μs phosphorescence lifetime measured for this suspension, the rate of quenching for the substrate is k_q = 3.87 × 10^8 M^{-1} s^{-1} (Figures 5 and S13). This rate is marginally slower than that previously measured for the homogeneous Ir(III) catalyzed system of 5.2 × 10^8 M^{-1} s^{-1}. Previously measured energetics of the carbon nitride excited state indicate that it is slightly less oxidizing (~1.57 V) than the excited state of $[Ir(dF(CF_3)ppy)_2(bpy)]PF_6$ (~1.67 V) dF(CF_3)ppy = 2-(2,4-difluorophenyl)-5-(trifluoromethyl)-pyridinyl, bpy = 2,2′-bipyridine),[51,52] which should result in a slightly slower electron transfer rate with equivalent mechanisms. In contrast to quenching in homogeneous systems, the long-lived emissive species in $^{NCN}CN_x^{148}$ cannot be fully quenched. Quenching of the emissive lifetime reaches a maximum after addition of only 2.4 mM substrate, at which point the lifetime of the long-lived state is less than two times shorter than the original lifetime (Figure S14). Further, exposing the $^{NCN}CN_x^{148}$ suspension to air resulted in a slightly higher quenching fraction, though the triplet state timescale remains distinct from that of the singlet (Figure 3B).

DISCUSSION

A triplet photochemistry emerges prominently in $^{NCN}CN_x$ with decreasing particle size. A long-lived and discrete triplet excited state allows for diffusive excited state quenching to occur and circumvents previous challenges in CN_x photochemistry arising from the asynchronicity of redox events driven out of trap states. We considered the possibility that the long-lived emissive state was the result of a thermally activated fluorescence process, which could return the exciton from a shallow trap or triplet dark state to an emissive singlet state. Whereas a delayed fluorescence would be expected to decrease in intensity as temperature is lowered, we observe an increase in emission intensity with decreasing temperature (Figure S10), indicating that the long-lived emission is not thermally activated. We therefore propose that the long-lived emission, with maximum intensity at ~475 nm, is phosphorescent in origin.

Heretofore, an outstanding challenge in elucidating CN_x photoactivity has been the absence of emission quenching upon the addition of substrates.[13,14,15] In the absence of emission quenching, mechanistic studies have emphasized the importance of kinetics associated with trap states, which have been used as a proxy for the reaction kinetics of the excited state of $^{NCN}CN_x$.[15] These long-lived trapped electrons can be competent for reactions requiring modest reducing potential, such as hydrogen evolution.[16] However, hole quenching kinetics are challenging to infer from an electronic trap state, and the accumulation of electrons in trap states results in faster charge recombination kinetics, further reducing the efficiency of photocatalytic processes using $^{NCN}CN_x$.[15] Additionally, driving photocatalysis out of trap states results in a thermodynamic penalty; the long-lived trap states in CN_x are considerably less reducing, with potentials estimated at –455 mV or deeper,[16,17] than the emissive conduction band (~–1120 mV) of ^{NCN}CN,[51] resulting in a significant energetic efficiency loss which may preclude use of CN_x materials for reactions requiring a substantial reduction potential.[53]

In line with previous studies monitoring the emission of CN_x materials on short timescales, which frequently report an absence of emissive quenching even when photocatalytic reactions driven by CN_x are occurring,[14,15] our initial experiments measuring steady-state photoluminescence also revealed no quenching using a

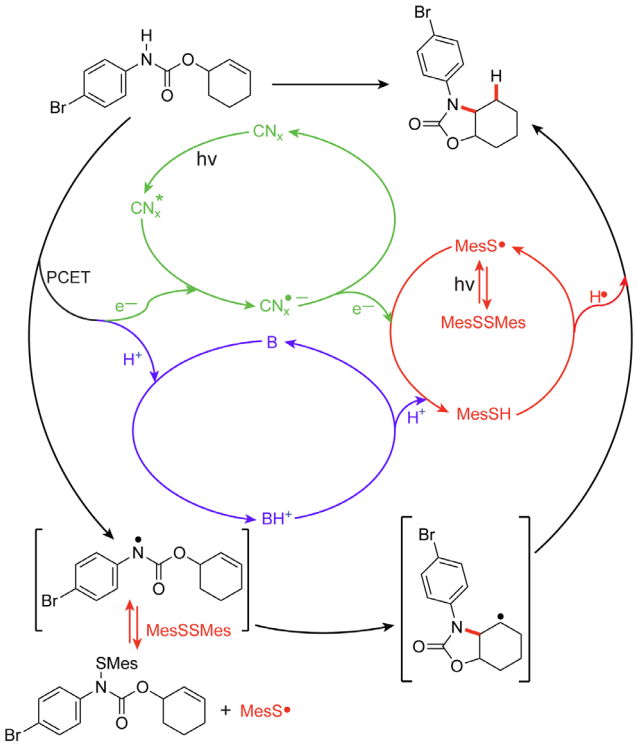

Figure 6. Mechanism of intramolecular hydroamidation catalyzed by CN_x, P_i^{Bu2} base (B), and bis(2,4,6-trimethylphenyl) disulfide (MesSSMes). Back reaction pathways are omitted.

combination of amide substrate and P_i^{Bu2}. This result (Figure S11) was in stark contrast to the strong emissive quenching caused by substrate and base for hydroamidation catalyzed by a homogeneous Ir(III) chromophore.[54] The observed absence of emissive quenching in steady-state measurements of $^{NCN}CN_x$ is due to the continued dominance of singlet fluorescence, which is too fast to be quenched by a process requiring diffusion of low concentration substrates. Time-resolved emission lifetime measurements allow us to separate the signals of the fast singlet fluorescence from the slower triplet emission. For the long-lived triplet, we observe emission lifetime quenching with the combination of amide substrate and phosphate base, resulting in the ability to derive electron transfer rates via standard mechanistic analyses. Thus, as a direct probe of the kinetics of the high energy excited state, triplet state emission quenching, rather than trap state quenching, provides a valuable mechanistic handle for photocatalysis using $^{NCN}CN_x$.

For many homogeneous photocatalysts, the addition of excess quencher results in complete emission quenching, resulting from a substantially faster rate of quenching than the rate of radiative relaxation. By contrast, with $^{NCN}CN_x$ we observe a plateau in the quenching fraction using amide and base. Further, even when using oxygen as a quencher the triplet emission remains on a distinct timescale from the singlet (Figure S14 and 3B). These results are consistent with an internal, non-solution accessible portion the long-lived excitons; they may be immobile within the $^{NCN}CN_x$ particle and are unable to be quenched at the solution interface. A population of internal excitons is also consistent with the observed increased reaction efficiency driven by smaller CN_x particles, which have a smaller fraction of excitons far from the surface.

The CN_x triplet state may be used to efficiently drive photoredox reactions, as demonstrated here for C–N bond formation from amides. Hydroamidation, and related hydroamination, driven by redox-neutral photocatalysis are powerful methods to forge C–N bonds,[38,39,55] with implications for a multitude of highly sought-after transformations, such as C–H activation[36,56] and selective deracemization.[57] Figure 6 shows the essential cycle for photo-hydroamidation. Initial oxidation by proton-coupled electron transfer (PCET) to generate an amidyl radical must be followed promptly by radical addition to an olefin. In order to complete the redox-neutral hydroamidation cycle and generate product, an H-atom must be returned to the cyclized substrate radical prior to competing back reactions.[54] Previous work in the homogeneously-catalyzed hydroamidation system has elucidated a dual role for the hydrogen atom transfer (HAT) catalysts 2,4,6-trimethylphenyl thiophenol (MesSH) or bis(2,4,6-trimethylphenyl) disulfide (MesSSMes) to both donate an H-atom to the substrate and to stabilize the intermediate radical reversibly by forming a transient thioamide to inhibit back electron transfer to the photocatalyst after initial substrate oxidation.[54] In the case here, MesSSMes plays a crucial role beyond circumventing the back electron transfer between $CN_x\bullet^-$ and the photogenerated amidyl radical (not shown in Figure 6). As indicated by the red cycle in Figure 6, MesSSMes provides a source of MesS•, which enters the catalytic HAT cycle, and in doing so supports the primary PCET chemistry of the CN_x photoredox cycle. However, the reduced $CN_x\bullet^-$ photocatalyst is not thermodynamically competent to reduce MesSSMes.[52,54] The direct photocleavage of MesSSMes to MesS• using 430 nm light (Figure S15) clarifies this mechanistic detail and thus allows for HAT to be established with MesS•, which accepts an electron from $CN_x\bullet^-$ and a proton from BH^+. To close the net redox-neutral cycle, the MesSH returns an H-atom to the cyclized substrate radical to form the hydroamidation product. Addition of MesSSMes rather than MesSH allows for an increased concentration of MesS•, which may be important for rapid electron extraction from $CN_x\bullet^-$ to avoid the buildup of trapped electrons which are known to accelerate charge recombination and impede efficient photocatalysis.[15]

The ability to tune the redox equivalency with CN_x particle size engenders superior photocatalytic activity. The overall efficiency of photo-hydroamidation reactions relying on molecular photocatalysts (e.g., $[Ir(dF(CF_3)ppy)_2(bpy)]^+$ is strongly dependent on the balance of forward and reverse rates for each step.[54] In contrast to homogeneous Ir(III) photocatalysts, for which each electron transfer event at the photocatalyst must be immediately and locally followed by an opposite redox event, CN_x can build up multiple electrons. In line with previous reports,[15,16] we observed a blue coloration of $^{NCN}CN_x$ during initial photo-hydroamidation screening reactions. This blue coloration indicates an imbalance in the rates of substrate oxidation versus thiyl radical reduction, thus allowing multiple substrate reductions to occur in series without corresponding thiyl radical reduction. By reducing the particle size, fewer electrons accumulate, leading to a balance in the rates of oxidation and reduction, promoting product formation rather than back reactions, thereby facilitating a closed redox photocycle.

CONCLUSIONS

Size reduction of $^{NCN}CN_x$ results in a prominent long-lived, emissive triplet excited state, which can enable photocatalytic processes requiring diffusive quenching. By directly utilizing the long-lived and high energy triplet excited state, redox-neutral, closed

photocycles may be achieved, as demonstrated herein for hydroamidation, resulting in substantially improved product yields. These results position CN_x materials favorably for further implementation as replacements for molecular photoredox catalysts. Beyond organic photoredox transformations, this work suggests that appropriately sized CN_x materials yield a triplet excited state that preludes a rich energy and electron transfer photochemistry.

ASSOCIATED CONTENT

Supporting Information

Experimental procedures, synthetic methods, materials characterization, and Figures S1-S15. The Supporting Information is available free of charge on the ACS Publications website.

AUTHOR INFORMATION

Corresponding Author

Daniel G. Nocera – Department of Chemistry and Chemical Biology, Harvard University, 12 Oxford Street, Cambridge, MA 02138–2902; orcid.org/0000-0001-5055-320X; E-mail: dnocera@fas.harvard.edu.

Author

Adam J. Rieth – Department of Chemistry and Chemical Biology, Harvard University, 12 Oxford Street, Cambridge, MA 02138–2902; orcid.org/0000-0002-9890-1346.

Yangzhong Qin – Department of Chemistry and Chemical Biology, Harvard University, 12 Oxford Street, Cambridge, MA 02138–2902; orcid.org/0000-0002-2450-521X.

Benjamin C. M. Martindale – Department of Chemistry and Chemical Biology, Harvard University, 12 Oxford Street, Cambridge, MA 02138–2902; orcid.org/0000-0002-7116-7989.

Funding Sources

This work was supported by the National Science Foundation under grant CHE-1855531. This work was performed in part at the Center for Nanoscale Systems (CNS), a member of the National Nanotechnology Coordinated Infrastructure Network (NNCI), which is supported by the National Science Foundation under NSF award no. 1541959. CNS is part of Harvard University.

REFERENCES

(1) Pauling, L.; Sturdivant, J. H. The Structure of Cyameluric Acid, Hydromelonic Acid and Related Substances. *Proc. Natl. Acad. Sci.* **1937**, *23*, 615–620.

(2) Wang, Y.; Vogel, A.; Sachs, M.; Sprick, R. S.; Wilbraham, L.; Moniz, S. J. A.; Godin, R.; Zwijnenburg, M. A.; Durrant, J. R.; Cooper, A. I.; Tang, J. Current Understanding and Challenges of Solar-Driven Hydrogen Generation Using Polymeric Photocatalysts. *Nat. Energy* **2019**, *4*, 746–760.

(3) Lau, V. W.; Moudrakovski, I.; Botari, T.; Weinberger, S.; Mesch, M. B.; Duppel, V.; Senker, J.; Blum, V.; Lotsch, B. V. Rational Design of Carbon Nitride Photocatalysts by Identification of Cyanamide Defects as Catalytically Relevant Sites. *Nat. Commun.* **2016**, *7* , 12165.

(4) Kasap, H.; Caputo, C. A.; Martindale, B. C. M.; Godin, R.; Lau, V. W. H.; Lotsch, B. V.; Durrant, J. R.; Reisner, E. Solar-Driven Reduction of Aqueous Protons Coupled to Selective Alcohol Oxidation with a Carbon Nitride-Molecular Ni Catalyst System. *J. Am. Chem. Soc.* **2016**, *138*, 9183–9192.

(5) Bajada, M. A.; Vijeta, A.; Savateev, A.; Zhang, G.; Howe, D.; Reisner, E. Visible-Light Flow Reactor Packed with Porous Carbon Nitride for Aerobic Substrate Oxidations. *ACS Appl. Mater. Interfac.* **2020**, *12* , 8176–8182.

(6) Cavedon, C.; Madani, A.; Seeberger, P. H.; Pieber, B. Semiheterogeneous Dual Nickel/Photocatalytic (Thio)Etherification Using Carbon Nitrides. *Org. Lett.* **2019**, *21*, 5331–5334.

(7) Pieber, B.; Malik, J. A.; Cavedon, C.; Gisbertz, S.; Savateev, A.; Cruz, D.; Heil, T.; Zhang, G.; Seeberger, P. H. Semi-Heterogeneous Dual Nickel/Photocatalysis Using Carbon Nitrides: Esterification of Carboxylic Acids with Aryl Halides. *Angew. Chem. Int. Ed.* **2019**, 9575–9580.

(8) Liu, Y.-Y.; Liang, D.; Lu, L.-Q.; Xiao, W.-J. Practical Heterogeneous Photoredox/Nickel Dual Catalysis for C–N and C–O Coupling Reactions. *Chem. Commun.* **2019**, *55* , 4853–4856.

(9) Khamrai, J.; Ghosh, I.; Savateev, A.; Antonietti, M.; König, B. Photo-Ni-Dual-Catalytic $C(sp^2)$–$C(sp^3)$ Cross-Coupling Reactions with Mesoporous Graphitic Carbon Nitride as a Heterogeneous Organic Semiconductor Photocatalyst. *ACS Catal.* **2020**, *10* , 3526–3532.

(10) Yang, C.; Li, R.; Zhang, K. A. I.; Lin, W.; Landfester, K.; Wang, X. Heterogeneous Photoredox Flow Chemistry for the Scalable Organosynthesis of Fine Chemicals. *Nat. Commun.* **2020**, *11*, 1–8.

(11) Qin, Y.; Martindale, B. C. M.; Sun, R.; Rieth, A. J.; Nocera, D. G. Solar-Driven Tandem Photoredox Nickel-Catalysed Cross-Coupling Using Modified Carbon Nitride. *Chem. Sci.* **2020**, *11*, 7456–7461.

(12) Zheng Y, Lin L, Wang B, Wang X. Graphitic Carbon Nitride Polymers toward Sustainable Photoredox Catalysis. *Angew. Chem. Int. Ed.* **2015**, 54. 12868–84.

(13) Lau, V. W.; Yu, V. W.; Ehrat, F.; Botari, T.; Moudrakovski, I.; Simon, T.; Duppel, V.; Medina, E.; Stolarczyk, J. K.; Feldmann, J.; Blum, V.; Lotsch, B. V. Urea-Modified Carbon Nitrides: Enhancing Photocatalytic Hydrogen Evolution by Rational Defect Engineering. *Adv. Energy Mater.* **2017**, *7* , 1–15.

(14) Kuriki, R.; Ranasinghe, C. S. K.; Yamazaki, Y.; Yamakata, A.; Ishitani, O.; Maeda, K. Excited-State Dynamics of Graphitic Carbon Nitride Photocatalyst and Ultrafast Electron Injection to a Ru(II) Mononuclear Complex for Carbon Dioxide Reduction. *J. Phys. Chem. C* **2018**, *122*, 16795–16802.

(15) Yang, W.; Godin, R.; Kasap, H.; Moss, B.; Dong, Y.; Hillman, S. A. J.; Steier, L.; Reisner, E.; Durrant, J. R. Electron Accumulation Induces Efficiency Bottleneck for Hydrogen Production in Carbon Nitride Photocatalysts. *J. Am. Chem. Soc.* **2019**, *141*, 11219–11229.

(16) Lau, V. W.; Klose, D.; Kasap, H.; Podjaski, F.; Pignié, M. C.; Reisner, E.; Jeschke, G.; Lotsch, B. V. Dark Photocatalysis: Storage of Solar Energy in Carbon Nitride for Time-Delayed Hydrogen Generation. *Angew. Chem. Int. Ed.* **2017**, *56*, 510–514.

(17) Godin, R.; Wang, Y.; Zwijnenburg, M. A.; Tang, J.; Durrant, J. R. Time-Resolved Spectroscopic Investigation of Charge Trapping in Carbon Nitrides Photocatalysts for Hydrogen Generation. *J. Am. Chem. Soc.* **2017**, *139*, 5216–5224.

(18) Cheng, H.; Xu, W. Recent Advances in Modified TiO_2 for Photo-induced Organic Synthesis. *Org. Biomol. Chem.* **2019**, *17*, 9977–9989.

(19) Zhao, W.; He, Z.; Tang, B. Z. Room-Temperature Phosphorescence from Organic Aggregates. *Nat. Rev. Mater.* **2020**, *5*, 869–885.

(20) Wang, H.; Jiang, S.; Liu, W.; Zhang, X.; Zhang, Q.; Luo, Y.; Xie, Y. Ketones as Molecular Co-Catalysts for Boosting Exciton-Based Photocatalytic Molecular Oxygen Activation. *Angew. Chem. Int. Ed.* **2020**, *59*, 11093–11100.

(21) Wang, H.; Jiang, S.; Chen, S.; Li, D.; Zhang, X.; Shao, W.; Sun, X.; Xie, J.; Zhao, Z.; Zhang, Q.; Tian, Y.; Xie, Y. Enhanced Singlet Oxygen Generation in Oxidized Graphitic Carbon Nitride for Organic Synthesis. *Adv. Mater.* **2016**, *28*, 6940–6945.

(22) Romero, N. A.; Nicewicz, D. A. Organic Photoredox Catalysis. *Chem. Rev.* **2016**, *116*, 10075–10166.

(23) Angnes, R. A.; Li, Z.; Correia, C. R. D.; Hammond, G. B. Recent Synthetic Additions to the Visible Light Photoredox Catalysis Toolbox. *Org. Biomol. Chem.* **2015**, *13*, 9152–9167.

(24) Twilton, J.; Le, C.; Zhang, P.; Shaw, M. H.; Evans, R. W.; MacMillan, D. W. C. The Merger of Transition Metal and Photocatalysis. *Nat. Rev. Chem.* **2017**, *1*, 0052.
(25) Shaw, M. H.; Twilton, J.; MacMillan, D. W. C. Photoredox Catalysis in Organic Chemistry. *J. Org. Chem.* **2016**, *8*, 6898–6926.
(26) Liang, Y.; Zhang, X.; MacMillan, D. W. C. Decarboxylative sp^3 C–N Coupling via Dual Copper and Photoredox Catalysis. *Nature* **2018**, *559*, 83–88.
(27) Ye, Y.; Sanford, M. S. Merging Visible-Light Photocatalysis and Transition-Metal Catalysis in the Copper-Catalyzed Trifluoromethyl-ation of Boronic Acids with CF_3 I. *J. Am. Chem. Soc.* **2012**, *134*, 9034–9037.
(28) Tellis, J. C.; Primer, D. N.; Molander, G. A. Single-Electron Transmetalation in Organoboron Cross-Coupling by Photoredox/Nickel Dual Catalysis. *Science* **2014**, *345*, 433–436.
(29) Beatty, J. W.; Stephenson, C. R. J. Amine Functionalization via Oxidative Photoredox Catalysis: Methodology Development and Complex Molecule Synthesis. *Acc. Chem. Res.* **2015**, *48*, 1474–1484.
(30) Zuo, Z.; Cong, H.; Li, W.; Choi, J.; Fu, G. C.; MacMillan, D. W. C. Enantioselective Decarboxylative Arylation of α-Amino Acids via the Merger of Photoredox and Nickel Catalysis. *J. Am. Chem. Soc.* **2016**, *138*, 1832–1835.
(31) Nicewicz, D. A.; MacMillan, D. W. C. Merging Photoredox Catalysis with Organocatalysis: The Direct Asymmetric Alkylation of Aldehydes. *Science* **2008**, *322*, 77–80.
(32) Rono, L. J.; Yayla, H. G.; Wang, D. Y.; Armstrong, M. F.; Knowles, R. R. Enantioselective Photoredox Catalysis Enabled by Proton-Coupled Electron Transfer: Development of an Asymmetric Aza-Pinacol Cyclization. *J. Am. Chem. Soc.* **2013**, *135*, 17735–17738.
(33) Loh, Y. Y.; Nagao, K.; Hoover, A. J.; Hesk, D.; Rivera, N. R.; Colletti, S. L.; Davies, I. W.; MacMillan, D. W. C. Photoredox-Catalyzed Deuteration and Tritiation of Pharmaceutical Compounds. *Science* **2017**, *358*, 1182–1187.
(34) Perry, I. B.; Brewer, T. F.; Sarver, P. J.; Schultz, D. M.; DiRocco, D. A.; MacMillan, D. W. C. Direct Arylation of Strong Aliphatic C–H Bonds. *Nature* **2018**, *560*, 70–75.
(35) Zhang, X.; MacMillan, D. W. C. Direct Aldehyde C–H Arylation and Alkylation via the Combination of Nickel, Hydrogen Atom Transfer, and Photoredox Catalysis. *J. Am. Chem. Soc.* **2017**, *139*, 11353–11356.
(36) Choi, G. J.; Zhu, Q.; Miller, D. C.; Gu, C. J.; Knowles, R. R. Catalytic Alkylation of Remote C–H Bonds Enabled by Proton-Coupled Electron Transfer. *Nature* **2016**, *539*, 268–271.
(37) Shaw, M. H.; Shurtleff, V. W.; Terrett, J. A.; Cuthbertson, J. D.; MacMillan, D. W. C. Native Functionality in Triple Catalytic Cross-Coupling: sp^3 C–H Bonds as Latent Nucleophiles. *Science* **2016**, *352*, 1304–1308.
(38) Miller, D. C.; Choi, G. J.; Orbe, H. S.; Knowles, R. R. Catalytic Olefin Hydroamidation Enabled by Proton-Coupled Electron Transfer. *J. Am. Chem. Soc.* **2015**, *137*, 13492–13495.
(39) Musacchio, A. J.; Lainhart, B. C.; Zhang, X.; Naguib, S. G.; Sherwood, T. C.; Knowles, R. R. Catalytic Intermolecular Hydroaminations of Unactivated Olefins with Secondary Alkyl Amines. *Science* **2017**, *355*, 727–730.
(40) Cheng, H.; Xu, W. Recent Advances in Modified TiO_2 for Photo-induced Organic Synthesis. *Org. Biomol. Chem.* **2019**, *17*, 9977–9989.
(41) Savateev, A.; Ghosh, I.; König, B.; Antonietti, M. Photoredox Catalytic Organic Transformations using Heterogeneous Carbon Nitrides. *Angew. Chem. Int. Ed.* **2018**, *57*, 15936–15947.
(42) Parrino, F.; Bellardita, M.; García-López, E. I.; Marcì, G.; Loddo, V.; Palmisano, L. Heterogeneous Photocatalysis for Selective Formation of High-value-added Molecules: Some Chemical and Engineering Aspects. *ACS Catal.* **2018**, *8*, 11191–11225.
(43) Kisch, H. Semiconductor Photocatalysis for Chemoselective Radical Coupling Reactions. *Acc. Chem. Res.* **2017**, *50*, 1002–1010.
(44) Ghosh, I.; Khamrai, J.; Savateev, A.; Shlapakov, N.; Antonietti, M.; König, B. Organic Semiconductor Photocatalyst Can Bifunctionalize Arenes and Heteroarenes. *Science* **2019**, *365*, 360–366.
(45) Jiang, Y.; Wang, C.; Rogers, C. R.; Kodaimati, M. S.; Weiss, E. A. Regio- and Diastereoselective Intermolecular [2+2] Cycloadditions Photocatalyzed by Quantum Dots. *Nat. Chem.* **2019**, *11*, 1034–1040.
(46) Zhu Q.; Nocera, D. G. Photocatalytic Hydromethylation and Hydroalkylation of Olefins Enabled by Titanium Dioxide Mediated Decarboxylation. *J. Am. Chem. Soc.* **2020**, *142*, 17913–17918.
(47) Bojdys, M. J.; Müller, J.-O.; Antonietti, M.; Thomas, A. Ionothermal Synthesis of Crystalline, Condensed, Graphitic Carbon Nitride. *Chem. Eur. J.* **2008**, *14*, 8177–8182.
(48) Zambon, A.; Mouesca, J. M.; Gheorghiu, C.; Bayle, P. A.; Pécaut, J.; Claeys-Bruno, M.; Gambarelli, S.; Dubois, L. S-Heptazine Oligomers: Promising Structural Models for Graphitic Carbon Nitride. *Chem. Sci.* **2016**, *7*, 945–950.
(49) Wang, X. L.; Fang, W. Q.; Yang, S.; Liu, P.; Zhao, H.; Yang, H. G. Structure Disorder of Graphitic Carbon Nitride Induced by Liquid-Assisted Grinding for Enhanced Photocatalytic Conversion. *RSC Adv.* **2014**, *4*, 10676–10679.
(50) Tauc, J.; Grigorovici, R.; Vancu, A. Optical Properties and Electronic Structure of Amorphous Germanium. *Phys. Status Solidi* **1966**, *15*, 627–637.
(51) Cao, S.; Low, J.; Yu, J.; Jaroniec, M. Polymeric Photocatalysts Based on Graphitic Carbon Nitride. *Adv. Mater.* **2015**, *27*, 2150–2176.
(52) Choi, G. J.; Knowles, R. R. Catalytic Alkene Carboaminations Enabled by Oxidative Proton-Coupled Electron Transfer. *J. Am. Chem. Soc.* **2015**, *137*, 9226–9229.
(53) Markushyna, Y.; Smith, C. A.; Savateev, A. Organic Photocatalysis: Carbon Nitride Semiconductors vs. Molecular Catalysts. *European J. Org. Chem.* **2020**, *2020*, 1294–1309.
(54) Ruccolo, S.; Qin, Y.; Schnedermann, C.; Nocera, D. G. General Strategy for Improving the Quantum Efficiency of Photoredox Hydroamidation Catalysis. *J. Am. Chem. Soc.* **2018**, *140*, 14926–14937.
(55) Musacchio, A. J.; Nguyen, L. Q.; Beard, G. H.; Knowles, R. R. Catalytic Olefin Hydroamination with Aminium Radical Cations: A Photoredox Method for Direct C–N Bond Formation. *J. Am. Chem. Soc.* **2014**, *136*, 12217–12220.
(56) Morton, C. M.; Zhu, Q.; Ripberger, H.; Troian-Gautier, L.; Toa, Z. S. D.; Knowles, R. R.; Alexanian, E. J. C–H Alkylation via Multisite-Proton-Coupled Electron Transfer of an Aliphatic C–H Bond. *J. Am. Chem. Soc.* **2019**, *141*, 13253–13260.
(57) Shin, N. Y.; Ryss, J. M.; Zhang, X.; Miller, S. J.; Knowles, R. R. Light - Driven Deracemization Enabled by Excited - State Electron Transfer. *Science* **2019**, *366*, 364–369.

Table of Contents